Cell. Mol. Biol. (ISSN: 1165-158X)

Journal Homepage: www.cellmolbiol.org

Cellular and Molecular Biology

Original Article

The therapeutic effects of ADSCs on photoaging of skin induced by UVB irradiation

Jing Wang#, Xiaochen Zhou#, Di Cao, Ying Meng, Yingchun Wang, Debin Yang*

Departments of Ultrasound, Jiading District Central Hospital Affiliated Shanghai University of Medicine & Health Sciences, Shanghai, China

Article Info

Article history:

Received: November 14, 2023
Accepted: February 22, 2024
Published: March 31, 2024

Use your device to scan and read the article online

Abstract

Skin photoaging affects appearance and is associated with a variety of skin diseases, even skin cancer. Therefore, the prevention and treatment of skin photoaging is very important. However, there is a lack of effective evaluation methods, so it is an urgent problem to explore a comprehensive, non-invasive and in vivo evaluation method. Adipose-derived mesenchymal stem cells (ADSCs) are widely used to improve skin conditions as easier to obtain and positive effects. Recently, as the development of ultrasound technology, skin ultrasound has been widely used. Changes in skin layer and structure can be observed by high-frequency ultrasound (HFUS). In addition, Shear wave elastography (SWE) technology can be used to monitor the change of skin hardness. However, it is necessary to further explore the ultrasound parameters in interpreting histological changes. We simulate the progression and treatment process of human skin photoaging by using UVB-induced nude mice skin photoaging model and ADSCs injection. The analysis of the degree and therapeutic effect of skin photoaging was conducted by HFUS, SWE and to verify with histopathology. Our study aims to clarify the value of HFUS combined SWE techniques in evaluating the degree and therapeutic efficacy of skin photoaging, which provides theoretical basis for diagnosis and treatment evaluation systems.

Keywords: ADSCs, Photoaging, UVB irradiation.

1. Introduction

Skin photoaging is a series of characteristic changes caused by excessively direct sun exposure, which is characterized by skin wrinkles, slackness, pigmentation or loss, and capillary expansion. Clinically, it is divided into two types: endogenous and exogenous skin photoaging. Notably, ultraviolet (UV) radiation, especially UVB, from the sunlight is the main cause of exogenous skin photoaging. Prolonged UVB radiation produces reactive oxygen species and free radicals accumulation, which in turn results in DNA damage, DNA synthesis disorder, and cell death [1, 2]. Besides, UVB radiation can generate inflammatory cytokines including IL-6, IL -2, IL-33, IL -8, TNF-α and IL-1, which accelerate skin aging [3]. In addition, UV exposure can also upregulate the expression of matrix metalloproteinases (MMPs) through various pathways. The upregulation of MMPs accelerates the degradation of collagen and normal elastin, as well as promotes the expression of abnormal elastin genes and the protein abnormal aggregation, which ultimately results in skin wrinkles and reduced elasticity [4-6]. Skin photoaging is associated with various skin diseases, even becoming a risk factor for precancerous lesions and skin cancers such as squamous cell carcinoma, and malignant melanoma [7]. Therefore, skin photoaging attracts high clinical attention. However, the means of therapy and evaluation of skin photoaging remain under further investigation.

Adipose-derived mesenchymal stem cells (ADSCs) are widely used to improve skin conditions as easier to obtain and have positive effects [8]. Park et al, first discovered that ADSCs can effectively improve wrinkle formation and dermal thickening in photoaging skin [9]. The anti-photoaging effect of ADSCs is mainly through secreting antioxidants and cytokines that act on corresponding target cells, which restrain oxidative stress and inflammatory response, promote collagen synthesis and stimulate human dermal fibroblasts (HDFs) proliferation, thereby improving a series of symptoms caused by skin photoaging damage [8, 10]. In addition, ADSCs can reverse the expression of MMP2, MMP13, phospho-NF-κB p65, Nlrp3, VCAM-1, α6 integrin, CD34, and collagen I induced by UVB radiation through the regulation of TGF-β2 in C57BL/6J mice [11]. Interestingly, Ichihashi et al reported that a single intradermal injection of autologous ADSCs rejuvenated aged facial skin and sharpened double eyelids. All the enrolled cases showed the shallowing and disappearance of wrinkles [12]. However, previous ADSCs experiments used pathological results as a means of evaluating efficacy, without dynamically observing the therapeutic effect. The evaluation of therapeutic effect and optimal action time

* Corresponding author.
E-mail address: yyddrr123@163.com (D. Yang).
# These authors contributed equally
Doi: http://dx.doi.org/10.14715/cmb/2024.70.3.35

is still lack of sufficient rapid, quantitative, accurate, and objective ways.

High-frequency ultrasound (HFUS) that uses sound waves greater than 20 MHz, characterized by non-invasive, inexpensive, real-time, repeatable and safe advantages, is used to measure skin aging and the effect of therapy [13, 14]. HFUS can identify the changes in skin thickness and echogenicity, including the throughout process of skin aging and therapy [15]. In addition, due to long-term exposure to sunlight, elastic degeneration of cutaneous papillary layer, collagen degradation, and accumulation of glycosaminoglycan form subepidermal low gyrus (SLEB). The SLEB occurrence and thickness can be used to infer the severity of skin photoaging [16]. With the increase of age, the relative echo of SLEB decreases and the thickness increases [13, 17]. Also, HFUS is proving to be an effective and indispensable technique for assessing skin photoaging [1, 18].

Elastic ultrasound (EUS), a type of ultrasonography, is used to evaluate tissue strain or stiffness based on the distinguishment in the various elasticities of different tissues. Even, EUS can identify the process of local physiological and pathological change [19, 20]. Shear wave elastography (SWE), as a type of EUS can obtain the value of Young's modulus by measuring the shear wave velocity, which quantitatively and qualitatively determines the hardness of tissue. In addition, there is a positive correlation between the value of Young's modulus and tissue hardness, which can accurately indicate the degree of tissue denaturation [21]. During the development of skin photoaging, not only the thickness of each layer of the skin change but also the normal elastic fibers decrease. Therefore, EUS can be used as an important means of examination for skin photoaging [22, 23].

Herein, we established UVB-induced nude mice skin photoaging model and ADSCs injection for simulating the progression and treatment process of human skin photoaging. HFUS and SWE in combination with histopathology were used to analyze the degree and therapeutic effect of skin photoaging. Our study provides theoretical basis in the system of early diagnosis and efficacy evaluation in skin photoaging.

2. Materials and methods

2.1. UVB radiation

The limbs of the model group mice were fixed and only the back skin was exposed. The mice were put in the UVB-skin photoaging chamber, in which the UVB lamp was placed at a vertical height of 28 cm above the mice and the radiation intensity was at the dose of 85 mJ/cm^2. The model group mice were exposed to UVB for 4 mins on alternate days. The skin changes of mice were observed every week during the irradiation period for erythema and ulceration. The mice in control group were fed conventionally without any intervention.

2.2. Animal studies

The female Balb/c nude mice (6-8 weeks, 15-20 g) were purchased from Jinan Pengyue Experimental animal Breeding company. All the mice were kept in the animal center with temperature of 20-24°C, the light and dark cycle of 12 h and a relative humidity of 40%-70%. All the mice were free of diet and water during the period of experiment.

2.3. Skin photoaging mouse model and grouping

The mice were randomly separated to 2 stages and each stage contained 4 groups. The groups in first stage were as follows: group 1, control group; group 2, UVB radiation for 6 weeks; group 3, UVB radiation for 8 weeks; group 4, UVB radiation for 10 weeks (n=4 per group). ADSCs of 5×10^6 in 80 μl were injected into the back of mice with water needle injection instrument every 10 days for 3 times. The groups in second stage were as follows: group 1, model group with UVB radiation for 8 weeks first and injection of normal saline three times; group 2, the ADSCs treatment group with UVB radiation for 8 weeks first and observation for 10 days after ADSCs injection; group 3, the ADSCs treatment group with UVB radiation for 8 weeks first and observation for 30 days after ADSCs injection; group 4, the ADSCs treatment group with UVB radiation for 8 weeks first and observation for 60 days after ADSCs injection (n=6 per group). The mice skin was photoed and performed ultrasonic inspection and measurement.

2.4. Ultrasonographic evaluation

The HFUS assessment of mice skin was performed with transducer frequency at 24 MHz by color Doppler echocardiography Aplio i900 (Canon, Japan). The limbs of mice were fixed on the test platform in prone position after the mice were anesthetized. A hydrogel pad was placed between the imaging site and the probe. The skin layers including the thickness of epidermis, dermis and subcutaneous tissue were measured longitudinally. For SWE measurement, the model was changed to SWE with transducer frequency at 18 MHz, which was used to evaluate the hardness of target skin, expressed by Young's value. All the measurements were repeated three times by the same sonographer with diagnostic expertise.

2.5. Grading of visible changes

The macroscopic features of the skin on the back of mice associated with photoaging (such as wrinkles, thickening, roughness, elasticity, erythema, etc.) were observed and evaluated, and the back skin was photographed and recorded. The skin on the back was evaluated according to the skin photoaging scoring criteria shown in Table 1, referred to Donald L's study and modification [24].

2.6. Measurement of skin elasticity

The elasticity of mice skin was evaluated twice every four weeks according to the method, described by Tsukahara et al. [25]. We used thumb and index finger to lift gently the rear position of the middle line of the back skin of the mouse with the mouse limbs not hanging in the air

Table 1. Grading scale of mouse skin photoaging.

Grade	Description of skin
0	No relaxation or wrinkles is observed; Normal skin texture is visible.
1	Fine wrinkles are visible.
2	A few light wrinkles are visible.
3	More light wrinkles are visible.
4	A few deep wrinkles and mild skin sagging are visible.
5	Deep wrinkles increased significantly.
6	Severe wrinkles; Skin damage occurs.

and immediately released. The time that the skin returned to its initial state was recorded.

2.7. Histological analysis

The mice back skin was collected. All the skin tissues were fixed in 4% paraformaldehyde and embedded in paraffin. Subsequently, the thickness at 5 μm section underwent hematoxylin-and eosin staining (Nanjing Jerry Biotechnology, Nanjing, China) to assess the change of skin tissue and the thickness of epidermis. The collagenous fiber distribution and morphology were detected by Massons staining (Nanjing Jerry Biotechnology, Nanjing, China). Weigert staining (Nanjing Jerry Biotechnology, Nanjing, China) was used to measure the distribution and morphology of elastic fibers. All the staining experiments were performed according to the instructions and previous studies [26]. The slides were photographed with light microscope.

2.8. Immunohistochemistry

The 5 μm section underwent immunohistochemistry using Ventana Benchmark Ultra Immunostainer (Roche, Basel, Switzerland) as previously described [27]. The primary antibody monoclonal rabbit anti-CD31 (Abcam, Cambridge, UK) and goat anti-rabbit IgG (Beyotime, Shanghai, China) were used according to the instructions. The slides were photographed with light microscope.

2.9. Western blotting

The total protein was extracted from the mice back skin with protein extract kit (Beyotime, Shanghai, China) according to the instructions. The protein quantification was performed using BCA protein assay kit (Beyotime, Shanghai, China). The samples (40 μg per sample) were separated by polyacrylamide gel electrophoresis. Subsequently, the protein was transferred to polyvinylidene fluoride membrane and blocked with 5% skim milk. The protein band was determined with Bio-Rad Molecular Imager (Bio-rad, Hercules, CA, USA) after the incubation of the first antibody Collagen I and GAPDH (Cloud-Clone Corp, China) and the secondary antibody: anti-rabbit IgG (Cloud-Clone Corp, China). Protein expression was quantified by Image J software (NIH, Bethesda, MD, USA).

2.10. Statistical analysis

All the data are presented as the mean ± standard deviation (mean ± SD). The statistical difference between groups was performed by one-way analysis of variance with GraphPad Prism 9 software (La Jolla, CA, USA). $P<0.05$ was considered as statistical significance. All the experiments were repeated at least three times.

3. Results

3.1. Comparison of visible changes in the back skin of mice

The UVB-radiation and nude mice were used to investigate the process of skin photoaging. In control group, the mice back skin presented normal skin texture with ruddy, delicate, glossy features. In contrast, the mice back skin in UVB-radiation group was rough, with anomalous thickening, partial light wrinkles and pigmentation at 6th week. Increased deep wrinkles, rough skin, dandruff, and even some leathery appearance can be observed in 8th and 10th week (Figure 1A). Accordingly, the skin photoaging score increased as the time of UVB radiation and the score in model group was higher than that in control group (Figure 1C). In addition, ADSCs treatment ameliorated the skin features and reversed the score induced by UVB and a significant difference was observed after ADSCs injection 10 days and 30 days (Figure 1B and D). These results showed that UVB-radiation of nude mice for skin photoaging model simulated the feature of natural skin aging successfully.

3.2. ADSCs reversed the reduction of skin elasticity induced by UVB

As depicted in Figure 2, there was no statistically significant difference in skin retraction recovery times between

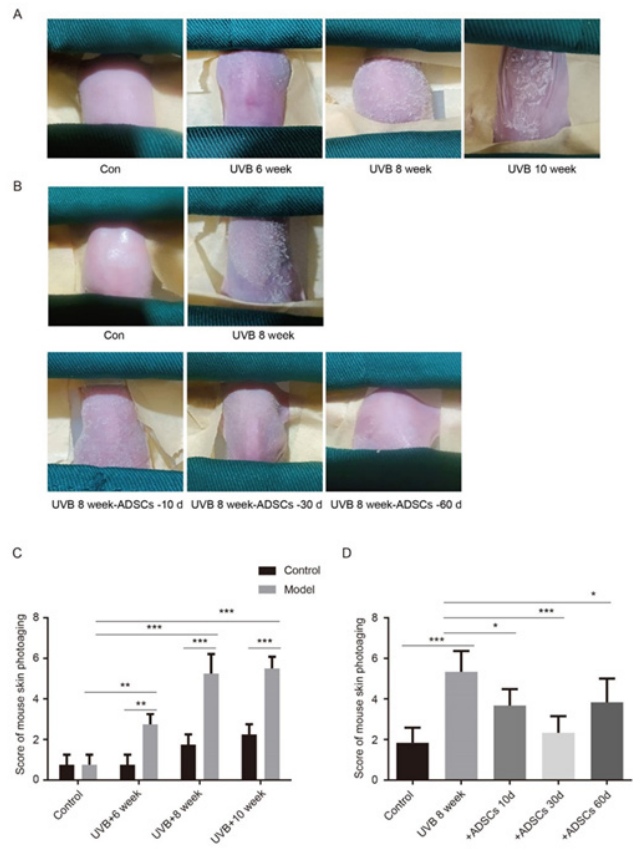

Fig. 1. Comparison of visible changes in the back skin of mice. (A) and (B) The back skin of mice appearance in control, UVB-radiation 6 weeks, 8 weeks, 10 weeks, and ADSCs treatment 10 days, 30 days and 60 days groups. (C) and (D) The skin photoaging score in control, UVB-radiation 6 weeks, 8 weeks, 10 weeks, and ADSCs treatment 10 days, 30 days and 60 days groups.

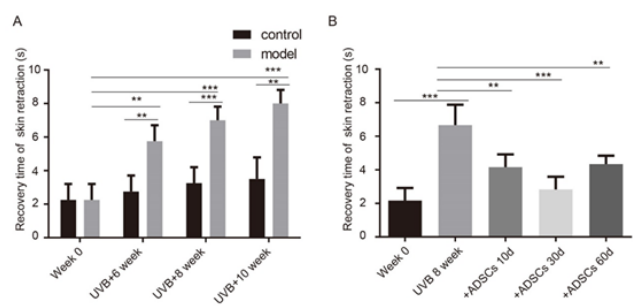

Fig. 2. ADSCs reversed the reduction of skin elasticity induced by UVB. (A) Skin retraction recovery times in the control and model groups (0, 6, 8 and 10 weeks). (B) Skin retraction recovery times in 0 week 0, 8 weeks, and ADSCs treatment groups.

the control and model groups at week 0. However, by weeks 6, 8 and 10, a significant divergence emerged, with the model group exhibiting a demonstrably longer skin recovery time compared to the control group (Figure 2A). However, ADSCs treatment decreased the skin recovery time and remarkably effective was observed after injection 30 days (Figure 2B). These findings provided compelling evidence that UVB radiation significantly diminished skin elasticity, thereby confirming the successful establishment of the nude mouse photoaging model.

3.3. ADSCs reversed the change of skin tissue structure and epidermal thickness induced by UVB

Histological analysis revealed distinct differences in skin tissue structure between the control and model groups. In control group, the epidermis was thin and uniform in thickness with normal stratum corneum, exhibiting no signs of excessive keratinization. The epidermal-Dermal Junction was clearly defined with a characteristic wavy pattern and showcased well-developed epidermal ridges and dermal papillae. The dermis was regularly arranged and structurally intact hair follicles and sebaceous glands, devoid of inflammatory infiltration or bleeding. Contrastly, in model group, the epidermis was irregularly thickened with excessive keratinization of the stratum corneum, indicative of photoaging. The epidermal-Dermal Junction was flattened and indistinct, with the disappearance of both epidermal ridges and dermal papillae (Figure 3A). Excitedly, ADSCs treatment ameliorated the UVB-induced skin damage (Figure 3B). The histopathological findings provided compelling evidence that UVB can induce significant structural changes in skin tissue, leading to photoaging and ADSCs can treat the skin damage induced by UVB.

3.4. ADSCs recovered the collagen fiber damage induced by UVB

Masson staining in UBV model group showed typical photoaging features, including a decrease in collagen fiber content, irregular and disordered arrangement, uneven distribution, and fragmentation or sparseness in some areas (Figure 4). In contrast, after ADSCs treatment, the collagen fibers in the skin tissue of photoaged mice showed a certain degree of recovery. Skin sections from the ADSCs 10 d and ADSCs 30 d groups showed wavy collagen fibers with uniform and orderly arrangement. The ADSCs 30 d group showed significant increase in collagen content. The skin sections from the ADSCs 60 d group showed wavy collagen fibers with regular and orderly arrangement and uniform distribution. These results suggested that ADSCs injection can alleviate collagen fiber damage caused by UVB irradiation in the early stage. The optimal effect was observed at around 30 days after ADSCs injection.

3.5. ADSCs recovered the elastic fibers damage induced by UVB

Weigert staining revealed a dose-dependent improvement in elastic fiber morphology in ADSCs-treated mice compared to the UVB group. The ADSCs10 d group exhibited thin, well-aligned elastic fibers, with some regions showcasing a woven-like pattern. Notably, the ADSCs 30 d group displayed significantly enhanced alignment, with areas even regaining a mesh-like structure, indicative of near-complete recovery. Conversely, the ADSCs 60 d group exhibited no significant improvement in alignment, with some areas showing irregular, granular, or amorphous deposits, suggesting incomplete restoration.

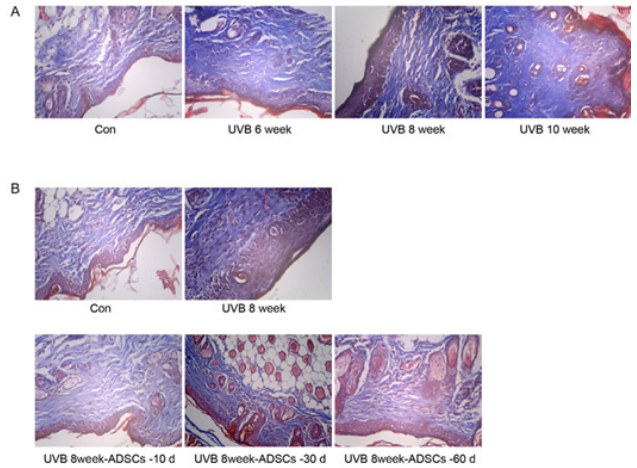

Fig. 4. ADSCs recovered the collagen fiber damage induced by UVB. (A) and (B) Masson staining analysis of mice back skin feature in control, UVB-radiation 6 weeks, 8 weeks, 10 weeks, and ADSCs treatment 10 days, 30 days and 60 days groups.

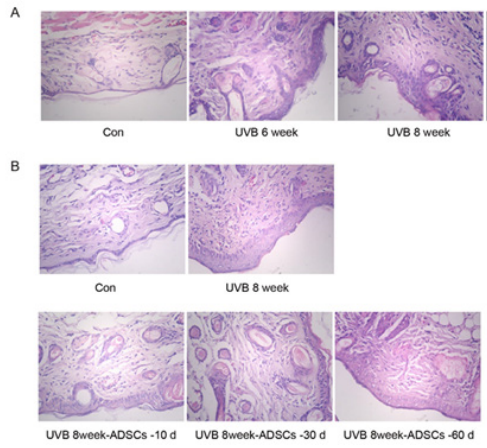

Fig. 3. ADSCs reversed the change of skin tissue structure and epidermal thickness induced by UVB. (A) and (B) Histological analysis of mice back skin feature in control, UVB-radiation 6 weeks, 8 weeks, 10 weeks, and ADSCs treatment 10 days, 30 days and 60 days groups.

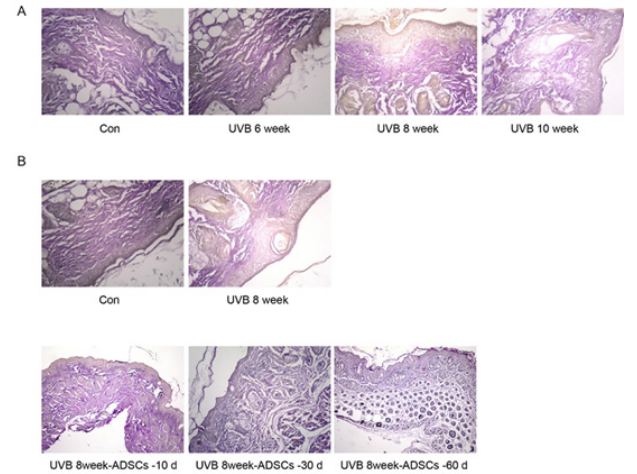

Fig. 5. ADSCs recovered the elastic fibers damage induced by UVB. (A) and (B) Weigert staining analysis of mice back skin feature in control, UVB-radiation 6 weeks, 8 weeks, 10 weeks, and ADSCs treatment 10 days, 30 days and 60 days groups.

These findings suggest that ADSCs injection can effectively ameliorate UVB-induced elastic fiber damage within the early window (around 30 days). ADSCs may act through promoting de novo elastic fiber production and/or facilitating the remodeling of damaged fibers (Figure 5).

3.6. ADSCs restored the angiogenesis inhibited by UVB

Immunohistochemistry for CD31 was used to evaluate the angiogenesis. Microvascular density (MVD) revealed UVB radiation inhibited the angiogenesis and ADSCs treatment recovered the angiogenesis in a dose-dependent (Figure 6A). Compared to the UVB group, both the ADSCs 10 d and ADSCs 30 d groups exhibited significantly elevated MVD (Figure 6B). This indicates a robust pro-angiogenic effect of ADSCs injection within the early stage (30 days) of photoaging. Interestingly, the ADSCs 60d group did not display a significant difference (Figure 6B). This suggested a potential response, where early ADSCs intervention effectively stimulated neovascularization, but the effect may diminish over time, requiring further investigation into optimal treatment timing for sustained microvascular benefits.

3.7. Evaluation of UVB-induced skin photoaging and ADSCs treatment efficacy using HFUS combined with SWE technology

HFUS combined with SWE technology showed that the thickness of the dermis and epidermis in the UVB model group was increased and dermal elasticity reduced compared to control group (Figure 7A-C). However, ADSCs treatment reversed the above results. After ADSCs treatment 10 d, 30 d, and 60 d, we found the thickness of the dermis and epidermis was decreased and dermal elasticity was reversed (Figure 7A-C). These results showed that HFUS combined with SWE technology is a promising technique for the assessment of skin photoaging.

3.8. ADSCs increased the collagen I expression inhibited by UVB

To further investigate the skin photoaging induced by UVB and the therapeutic effect of ADSCs. We detected the collagen I expression in protein level by Westen blotting. The results showed that collagen I expression exhibited a significant decline in the UVB groups in weeks 6, 8 and 10, indicative of photoaging-induced collagen depletion (Figure 8A and B). However, Collagen-I protein expression significantly increases in the ADSCs 10 d, ADSCs 30 d, and ADSCs 60 d groups compared to the UVB group in a dose-dependent manner. Notably, the ADSCs 30 d group displayed the highest Collagen-I content, suggesting a

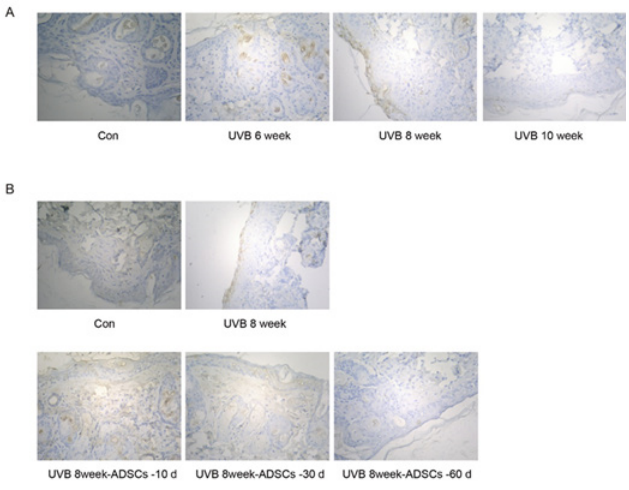

Fig. 6. ADSCs restored the angiogenesis inhibited by UVB. (A) and (B) The evaluation of the angiogenesis using CD31 staining by immunohistochemistry in control, UVB-radiation 6 weeks, 8 weeks, 10 weeks, and ADSCs treatment 10 days, 30 days and 60 days groups.

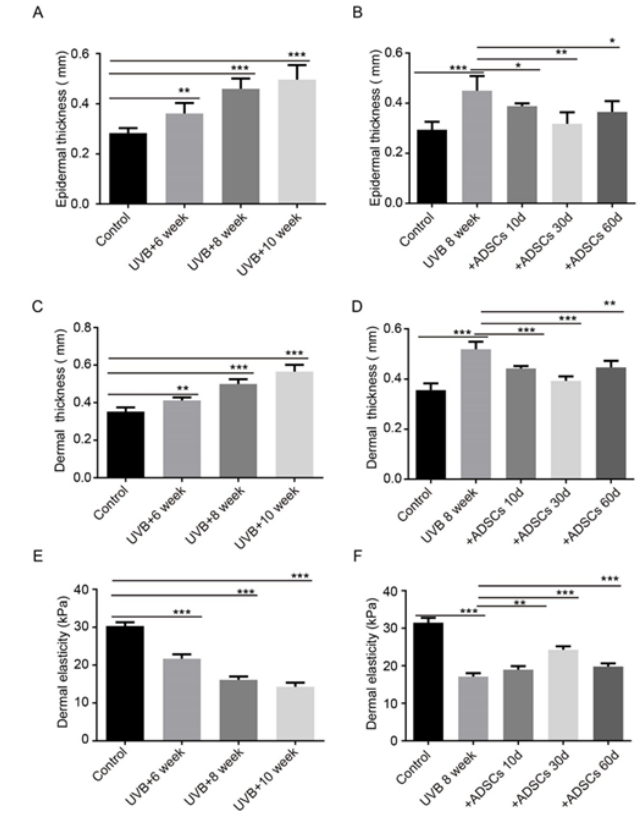

Fig. 7. Evaluation of UVB-induced skin photoaging and ADSCs treatment efficacy using HFUS combined with SWE technology. (A) Evaluation of epidermis thickness in control, UVB-radiation 6 weeks, 8 weeks, 10 weeks, and ADSCs treatment 10 days, 30 days and 60 days groups using HFUS combined with SWE technology. (B) Evaluation of dermis thickness in control, UVB-radiation 6 weeks, 8 weeks, 10 weeks, and ADSCs treatment 10 days, 30 days and 60 days groups using HFUS combined with SWE technology. (C) Evaluation of dermal elasticity in control, UVB-radiation 6 weeks, 8 weeks, 10 weeks, and ADSCs treatment 10 days, 30 days and 60 days groups using HFUS combined with SWE technology.

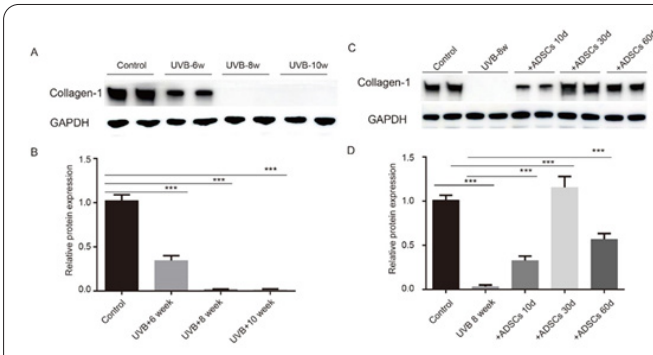

Fig. 8. ADSCs increased the collagen I expression inhibited by UVB. (A) and (B) The expression of collagen I in control, UVB-radiation 6 weeks, 8 weeks and 10 weeks groups, detected by Western blot and quantization. (C) and (D) The expression of collagen I in control, 8 weeks and ADSCs treatment 10 days, 30 days and 60 days groups, detected by Western blot and quantization.

peak recovery window at 30 days post-injection (Figure 8C and D). These findings demonstrated that ADSCs injection can effectively restore Collagen-I levels in photoaged skin, offering promising therapeutic potential for combating photoaging effects.

4. Discussion

Our study verified that UVB radiation can simulate skin photoaging and ADSCs treatment reversed the skin damage induced by UVB. We used the combination of HFUS and SWE technology to detect the change in skin thickness and elasticity, which was consistent with histological analysis and molecular level analysis. This study developed a non-invasive, and in vivo method for evaluating skin photoaging.

As we all know, UVB is the primary extrinsic cause of skin photoaging. In our study, we observed the mice skin was rough, with anomalous thickening, wrinkling and pigmentating as UVB radiation time. Besides, UVB radiation exhibited a longer skin recovery compared to control mice. Histological analysis showed epidermal alterations were evident in irregular thickening with excessive stratum corneum keratinization and diminished epidermal ridges and dermal papillae. The presence of bleeding and extensive inflammatory cell infiltration within the dermis provided further confirmation. Masson staining and Weigert staining demonstrated that collagen fiber and elastic fiber presented irregular and disordered arrangements. At the molecular level, Westen Blotting showed collagen I expression was significantly decreased. The HFUS combined with SWE technology also indicated the increased thickness of the dermis and epidermis and decreased dermal elasticity. All the above results were consistent with previous study [28-30], which indicated we established that skin photoaging successfully and UVB radiation can cause a series of damage to the skin. ADSCs were reported that injection of ADSCs can reverse skin photoaging by various studies

Gao et al. showed that LncRNA H19 from the exosome of ADSCs supernatant can inhibit UVB-induced skin photoaging by upregulation of SIRT1 via miR-138 [31]. Also, extracellular vesicles from ADSCs can decrease ROS accumulation and the inflammatory response, which relieves skin photoaging [32]. Similarly, our results also showed that ADSCs treatment decreased the UVB-induced skin photoaging damage, which was characterized by visible changes in mice back skin, skin elasticity, skin tissue structure, thickness, angiogenesis, collagen fiber, elastic fibers, and collagen I expression. In this study, we also found the time of ADSCs treatment was very important. Despite promising results, current ADSCs research lacks robust methods for dynamically monitoring therapeutic effects. The critical need for rapid, quantitative, accurate, and objective evaluation tools remains unmet, hindering the optimization of treatment timing and efficacy assessment.

In recent years, non-invasive diagnostic detection methods based on optics, electrics, and electromagnetics have been applied in the evaluation of skin photoaging more widely. Dermoscope, as a noninvasive technique for examining skin diseases, is used to evaluate photoaging, which only detects the vascular and pigment changes that were limited to epidermis and superficial dermis [33]. Optical Coherence Tomography (OCT) can be used to assess upper dermal degeneration and skin photoaging roughness and wrinkle formation, but OCT is expensive and the equipment is in high required [34]. In contrast, HFUS is a non-invasive imaging technique that can be used to assess skin photoaging. HFUS uses high-frequency sound waves to generate images of the skin and measure the thickness, elasticity, collagen content and other features of the skin [35]. SWE can specifically quantify tissue elasticity by generating and analyzing shear waves. SWE-derived parameters for skin photoaging assessment include Young's modulus, shear wave velocity (SWV) and tissue damping [36-38]. Therefore, HFUS combined with SWE technology is a promising technique for the comprehensive assessment of skin aging. In our study, by using the method of HFUS combined with SWE technology, we observed UVB radiation resulted in the increasing thickness of skin and decreasing skin elasticity and ADSCs treatment reversed the skin damage. This evaluation was consistent with histological analysis and molecular-level analysis. In addition, to investigate the therapeutical effect of ADSCs for UVB-induced skin photoaging, the specific molecular mechanisms remain to explore further. Also, the assessment methods for skin photoaging need to much research.

5. Conclusion

Our study confirmed that UVB radiation can induce skin photoaging and ADSCs treatment reversed the skin photoaging damage induced by UVB. We explored the role of HFUS combined with SWE technology in early diagnosis and efficacy evaluation of skin photoaging. The examination technique is non-invasive, efficient and accurate, which is expected to provide a basis for the evaluation of the disease progression and treatment prognosis of skin photoaging.

Conflict of interests

The author has no conflicts with any step of the article preparation.

Consent for publications

The author read and approved the final manuscript for publication.

Ethics approval and consent to participate

This study was approved by the Animal Ethics Committee of Shanghai University of Medicine & Health Sciences Animal Center.

Informed consent

The authors declare not used any patients in this research.

Availability of data and material

The data that support the findings of this study are available from the corresponding author upon reasonable request

Authors' contributions

Jing Wang, Xiaochen Zhou: Conceptualization, methodology, writing original draft preparation. Di Cao, Ying Meng, Yingchun Wang: Investigation, software, statistical analysis. Debin Yang: Reviewing and editing, funding acquisition, supervision. All authors read and approved the final manuscript.

Funding

This work was supported by the Project of Jiading District Health Commission of Shanghai, No.2022-KY-09; Key Medical Specialty Project of Jiading District, Shanghai (No.2020-jdyxzdzk-02)

References

1. Chiu HW, Chen CH, Chen YJ, Hsu YH (2017) Far-infrared suppresses skin photoaging in ultraviolet B-exposed fibroblasts and hairless mice. Plos One 12:e0174042. doi: 10.1371/journal.pone.0174042
2. Kim J, Lee N, Chun YS, Lee SH, Ku SK (2023) Krill Oil's Protective Benefits against Ultraviolet B-Induced Skin Photoaging in Hairless Mice and In Vitro Experiments. Mar Drugs 21:479 doi: 10.3390/md21090479
3. Titisari RS, Herawati E, Astirin OP (2023) Oral intake of collagen hydrolysate from mackerel scad (Decapterus macarellus) attenuates skin photoaging by suppressing the UVB-induced expression of MMP-1 and IL-6. J Complement Integr Med doi: 10.1515/jcim-2023-0209
4. Thapa MT, Mallik SK, Gurung P, Lim J, Kim YT, Shrestha R et al (2023) Chlorin E6-Curcumin-Mediated Photodynamic Therapy Promotes an Anti-Photoaging Effect in UVB-Irradiated Fibroblasts. Int J Mol Sci 24:13468. doi: 10.3390/ijms241713468
5. Shu P, Li M, Zhao N, Wang Y, Zhang L, Du Z (2023) Efficacy and mechanism of retinyl palmitate against UVB-induced skin photoaging. Front Pharmacol 14:1278838. doi: 10.3389/fphar.2023.1278838
6. Fan Z, Zhou Y, Gan B, Li Y, Chen H, Peng X et al (2023) Collagen-EGCG Combination Synergistically Prevents UVB-Induced Skin Photoaging in Nude Mice. Macromol Biosci 23:e2300251. doi: 10.1002/mabi.202300251
7. Stoffels I, Morscher S, Helfrich I, Hillen U, Leyh J, Burton NC et al (2015) Metastatic status of sentinel lymph nodes in melanoma determined noninvasively with multispectral optoacoustic imaging. Sci Transl Med 7:317ra199. doi: 10.1126/scitranslmed.aad1278
8. Won CH, Park GH, Wu X, Tran TN, Park KY, Park BS et al (2017) The Basic Mechanism of Hair Growth Stimulation by Adipose-derived Stem Cells and Their Secretory Factors. Curr Stem Cell Res T 12:535-543. doi: 10.2174/1574888X12666170829161058
9. Park BS, Jang KA, Sung JH, Park JS, Kwon YH, Kim KJ et al (2008) Adipose-derived stem cells and their secretory factors as a promising therapy for skin aging. Dermatol Surg 34:1323-1326. doi: 10.1111/j.1524-4725.2008.34283.x
10. Liang JX, Liao X, Li SH, Jiang X, Li ZH, Wu YD et al (2020) Antiaging Properties of Exosomes from Adipose-Derived Mesenchymal Stem Cells in Photoaged Rat Skin. Biomed Res Int 2020:6406395. doi: 10.1155/2020/6406395
11. Gong M, Zhai X, Yu L, Li C, Ma X, Shen Q et al (2020) ADSCs inhibit photoaging- and photocarcinogenesis-related inflammatory responses and extracellular matrix degradation. J Cell Biochem 121:1205-1215. doi: 10.1002/jcb.29354
12. Ichihashi M, Tanaka M, Iizuka T, Totsuka H, Tominaga E, Hitomi Y et al (2023) A Single Intradermal Injection of Autologous Adipose-Tissue-Derived Stem Cells Rejuvenates Aged Skin and Sharpens Double Eyelids. J Pers Med 13:1162. doi: 10.3390/jpm13071162
13. Vergilio MM, Vasques LI, Leonardi GR (2021) Characterization of skin aging through high-frequency ultrasound imaging as a technique for evaluating the effectiveness of anti-aging products and procedures: A review. Skin Res Technol 27:966-973. doi: 10.1111/srt.13033
14. Vergilio MM, Aiello LM, Furlan AS, Carita AC, Azevedo JR, Bolzinger MA et al (2022) In vivo evaluation of topical ascorbic acid application on skin aging by 50 MHz ultrasound. J Cosmet Dermatol-Us 21:4921-4926. doi: 10.1111/jocd.14892
15. Crisan D, Lupsor M, Boca A, Crisan M, Badea R (2012) Ultrasonographic assessment of skin structure according to age. Indian J Dermatol Ve 78:519. doi: 10.4103/0378-6323.98096
16. Vergilio MM, Monteiro ESS, Vasques LI, Leonardi GR (2021) Characterization of women's young and mature skin by the 50 MHz high-frequency ultrasound technique. J Cosmet Dermatol-Us 20:3695-3697. doi: 10.1111/jocd.13999
17. Firooz A, Rajabi-Estarabadi A, Zartab H, Pazhohi N, Fanian F, Janani L (2017) The influence of gender and age on the thickness and echo-density of skin. Skin Res Technol 23:13-20. doi: 10.1111/srt.12294
18. Mlosek RK, Migda B, Migda M (2021) High-frequency ultrasound in the 21(st) century. J Ultrason 20:e233-e241. doi: 10.15557/JoU.2020.0042
19. Ambroziak M, Pietruski P, Noszczyk B, Paluch L (2019) Ultrasonographic elastography in the evaluation of normal and pathological skin - a review. Postep Derm Alergol 36:667-672. doi: 10.5114/ada.2018.77069
20. Ophir J, Garra B, Kallel F, Konofagou E, Krouskop T, Righetti R et al (2000) Elastographic imaging. Ultrasound Med Biol 26 Suppl 1:S23-S29. doi: 10.1016/s0301-5629(00)00156-3
21. Sigrist R, Liau J, Kaffas AE, Chammas MC, Willmann JK (2017) Ultrasound Elastography: Review of Techniques and Clinical Applications. Theranostics 7:1303-1329. doi: 10.7150/thno.18650
22. Luo CC, Qian LX, Li GY, Jiang Y, Liang S, Cao Y (2015) Determining the in vivo elastic properties of dermis layer of human skin using the supersonic shear imaging technique and inverse analysis. Med Phys 42:4106-4115. doi: 10.1118/1.4922133
23. Ambroziak M, Noszczyk B, Pietruski P, Guz W, Paluch L (2019) Elastography reference values of facial skin elasticity. Postep Derm Alergol 36:626-634. doi: 10.5114/ada.2018.77502
24. Bissett DL, Hannon DP, Orr TV (1987) An animal model of solar-aged skin: histological, physical, and visible changes in UV-irradiated hairless mouse skin. Photochem Photobiol 46:367-378. doi: 10.1111/j.1751-1097.1987.tb04783.x
25. Tsukahara K, Moriwaki S, Hotta M, Fujimura T, Sugiyama-Nakagiri Y, Sugawara S et al (2005) The effect of sunscreen on skin elastase activity induced by ultraviolet-A irradiation. Biol Pharm Bull 28:2302-2307. doi: 10.1248/bpb.28.2302
26. Li S, Sun J, Yang J, Yang Y, Ding H, Yu B et al (2023) Gelatin methacryloyl (GelMA) loaded with concentrated hypoxic pretreated adipose-derived mesenchymal stem cells(ADSCs) conditioned medium promotes wound healing and vascular regeneration in aged skin. Biomater Res 27:11. doi: 10.1186/s40824-023-00352-3
27. Rauchenwald T, Handle F, Connolly CE, Degen A, Seifarth C, Hermann M et al (2023) Preadipocytes in human granulation tissue: role in wound healing and response to macrophage polarization. Inflamm Regen 43:53. doi: 10.1186/s41232-023-00302-5
28. Dirat B, Samouillan V, Dandurand J, Gardou JP, Walter V, Santran V (2023) Positive effects of hypoxic preconditioning of the extracellular matrix and stromal vascular fraction from adipose tissue. Jpras Open 38:173-185. doi: 10.1016/j.jpra.2023.09.007
29. Qu L, Wang F, Ma X (2023) The extract from Portulaca oleracea L. rehabilitates skin photoaging via adjusting miR-138-5p/Sirt1-mediated inflammation and oxidative stress. Heliyon 9:e21955. doi: 10.1016/j.heliyon.2023.e21955
30. Xu P, Yu Q, Huang H, Zhang WJ, Li W (2018) Nanofat Increases Dermis Thickness and Neovascularization in Photoaged Nude Mouse Skin. Aesthet Plast Surg 42:343-351. doi: 10.1007/

s00266-018-1091-4

31. Gao W, Zhang Y, Yuan L, Huang F, Wang YS (2023) Long Noncoding RNA H19-Overexpressing Exosomes Ameliorate UVB-Induced Photoaging by Upregulating SIRT1 Via Sponging miR-138. Photochem Photobiol 99:1456-1467. doi: 10.1111/php.13801
32. Xu P, Xin Y, Zhang Z, Zou X, Xue K, Zhang H et al (2020) Extracellular vesicles from adipose-derived stem cells ameliorate ultraviolet B-induced skin photoaging by attenuating reactive oxygen species production and inflammation. Stem Cell Res Ther 11:264. doi: 10.1186/s13287-020-01777-6
33. Hu SC, Lin CL, Yu HS (2019) Dermoscopic assessment of xerosis severity, pigmentation pattern and vascular morphology in subjects with physiological aging and photoaging. Eur J Dermatol 29:274-280. doi: 10.1684/ejd.2019.3555
34. Mamalis A, Ho D, Jagdeo J (2015) Optical Coherence Tomography Imaging of Normal, Chronologically Aged, Photoaged and Photodamaged Skin: A Systematic Review. Dermatol Surg 41:993-1005. doi: 10.1097/DSS.0000000000000457
35. Tao Y, Wei C, Su Y, Hu B, Sun D (2022) Emerging High-Frequency Ultrasound Imaging in Medical Cosmetology. Front Physiol 13:885922. doi: 10.3389/fphys.2022.885922
36. Popova V, Botushanov A, Batalov Z, Karalilova R, Batalov A (2023) High-resolution musculoskeletal ultrasonography and elastography for eosinophilic fasciitis diagnosis and follow-up: a case-based review. Rheumatol Int 43:2311-2318. doi: 10.1007/s00296-023-05401-7
37. Turk CB, Baykara UM, Dos YM, Manav BV, Sarikaya TE, Koku AA (2023) The Effects of Oral Isotretinoin on Atrophic Acne Scars Measured by Shear-wave Elastography: An Observational, Single-center Study. J Clin Aesthet Dermatol 16:46-51.
38. Paluch L, Ambroziak M, Pietruski P, Noszczyk B (2019) Shear Wave Elastography in the Evaluation of Facial Skin Stiffness After Focused Ultrasound Treatment. Dermatol Surg 45:1620-1626. doi: 10.1097/DSS.0000000000001881